

# UC Irvine

## UC Irvine Previously Published Works

### Title

Chemical kinetics of multiphase reactions between ozone and human skin lipids: Implications for indoor air quality and health effects

### Permalink

<https://escholarship.org/uc/item/82933277>

### Journal

Indoor Air, 27(4)

### ISSN

0905-6947

### Authors

Lakey, PSJ  
Wisthaler, A  
Berkemeier, T  
et al.

### Publication Date

2017-07-01

### DOI

10.1111/ina.12360

Peer reviewed

## ORIGINAL ARTICLE

# Chemical kinetics of multiphase reactions between ozone and human skin lipids: Implications for indoor air quality and health effects

P. S. J. Lakey<sup>1</sup> | A. Wisthaler<sup>2</sup> | T. Berkemeier<sup>1</sup> | T. Mikoviny<sup>2</sup> | U. Pöschl<sup>1</sup> | M. Shiraiwa<sup>1,3</sup>

<sup>1</sup>Multiphase Chemistry Department, Max Planck Institute for Chemistry, Mainz, Germany

<sup>2</sup>Department of Chemistry, University of Oslo, Oslo, Norway

<sup>3</sup>Department of Chemistry, University of California, Irvine, CA, USA

**Correspondence**

M. Shiraiwa, Department of Chemistry, University of California, Irvine, CA, USA.  
Email: m.shiraiwa@uci.edu

**Funding information**

Max-Planck-Gesellschaft; Max Planck Graduate Center with the Johannes Gutenberg-Universität Mainz (MPGC)

**Abstract**

Ozone reacts with skin lipids such as squalene, generating an array of organic compounds, some of which can act as respiratory or skin irritants. Thus, it is important to quantify and predict the formation of these products under different conditions in indoor environments. We developed the kinetic multilayer model that explicitly resolves mass transport and chemical reactions at the skin and in the gas phase (KM-SUB-Skin). It can reproduce the concentrations of ozone and organic compounds in previous measurements and new experiments. This enabled the spatial and temporal concentration profiles in the skin oil and underlying skin layers to be resolved. Upon exposure to ~30 ppb ozone, the concentrations of squalene ozonolysis products in the gas phase and in the skin reach up to several ppb and on the order of ~10 mmol m<sup>-3</sup>. Depending on various factors including the number of people, room size, and air exchange rates, concentrations of ozone can decrease substantially due to reactions with skin lipids. Ozone and dicarbonyls quickly react away in the upper layers of the skin, preventing them from penetrating deeply into the skin and hence reaching the blood.

**KEYWORDS**

dicarbonyls, kinetic modeling, ozone, respiratory irritants, skin irritants, squalene

## 1 | INTRODUCTION

People spend on average 90% of their time indoors. Indoor air can be more polluted than outdoor air and the World Health Organization estimated that in 2002 indoor air pollution was responsible for 1.5 million deaths and 2.7% of the global burden of disease.<sup>1</sup> Therefore, better understanding of the air quality and reactions that can occur within indoor environments is very important. A major oxidant that has been measured in indoor environments is O<sub>3</sub> with concentrations inside buildings and houses ranging between ~5 and 150 ppb.<sup>2</sup> O<sub>3</sub> can be inhaled by people as well as reacting with indoor furnishings, cleaning products, and the skin oils of the occupants within the building.<sup>3–6</sup> Human skin oils contain many unsaturated species that are reactive toward O<sub>3</sub> including squalene, fatty acids, wax esters, sterols, glycerols, phospholipids as well as antioxidants (ascorbate, uric acid, glutathione, and α-tocopherol), and coenzyme Q.<sup>7–10</sup>

Interactions of O<sub>3</sub> with skin lipids are important for indoor air quality, including O<sub>3</sub> concentration and deposition in an indoor environment.<sup>11–13</sup> The reaction of O<sub>3</sub> with skin oils has previously been investigated in enclosed spaces such as aircraft cabins and simulated offices by exposing people, hair, or soiled clothing.<sup>6,14–20</sup> These studies have consistently shown that the presence of human occupants and soiled clothes will decrease O<sub>3</sub> concentrations substantially within the enclosed space, whilst volatile species will increase in the gas phase. These volatile products, especially the dicarbonyls, have the potential to be respiratory irritants.<sup>21,22</sup> The composition and concentration of secondary organic aerosol (SOA), an important fraction of indoor particulate matter, would also be impacted by changes in O<sub>3</sub> concentrations and volatile organic compounds (VOCs).<sup>15,23–25</sup>

Squalene ozonolysis products have also been observed to accumulate in skin oil that has been exposed to ozone.<sup>26</sup> These lower volatility products may be skin irritants and could also be absorbed into the

bloodstream over time.<sup>21,27,28</sup> Several models of the skin exist, focusing on dermal absorption from the gas phase.<sup>29,30</sup> For example, Gong et al. predicted the absorption rate of six different phthalate esters into the blood when skin was exposed to these gas-phase species for varying amounts of time.<sup>29</sup> However, currently to our knowledge, these skin models have not combined physical processes (adsorption, desorption, and diffusion) with chemistry. Our aim was to develop a model to estimate the concentrations of  $O_3$  and respiratory and skin irritants formed upon exposure of people to  $O_3$  in different indoor environments.

## 2 | DESCRIPTION OF THE KM-SUB-SKIN MODEL

The kinetic multilayer model of surface and bulk chemistry of the skin (KM-SUB-Skin) was developed based on the kinetic multilayer model for aerosol surface and bulk chemistry (KM-SUB).<sup>31</sup> A schematic of processes occurring in KM-SUB-Skin is shown in Figure 1. The model includes different layers: a gas phase, a near-surface gas phase, a sorption layer, a skin oil layer, a number of bulk layers in the stratum corneum and in the viable epidermis, and a layer of blood vessels. The skin is assumed to be uniformly covered by  $\sim 0.45\text{-}\mu\text{m}$ -thick skin oil.<sup>32</sup> It should also be noted that there is some variability in the skin oil thickness of a person and skin oil concentrations in different regions of the body.<sup>32-34</sup> This would affect the concentrations of both ozone and the squalene ozonolysis products, as there would be more squalene molecules for ozone to react with. Sensitivity tests showed that a variability of skin oil thickness would not affect the predicted concentrations in the skin and fluxes into the blood significantly (see Supporting Information).

### Practical implications

- Reactions of ozone with skin lipids in indoor environments impact indoor air quality by decreasing ozone concentrations and increasing concentrations of squalene ozonolysis products in the gas phase. These products include monocarbonyls and dicarbonyls, which are likely to be respiratory and skin irritants. Monocarbonyls can diffuse through the skin and enter the blood, potentially causing adverse health effects. We have developed a model to quantify skin ozonolysis products in different indoor environments.

The stratum corneum is the outermost part of the skin and consists of 15-20 layers of dead flattened cells with a thickness of  $\sim 25\ \mu\text{m}$ .<sup>35</sup> The viable epidermis is the skin below the stratum corneum and consists of living cells with a thickness of  $\sim 100\ \mu\text{m}$ .<sup>36</sup> In this study, both parts were described with 20 bulk layers. The model treats the following mass transport and chemical reactions explicitly: adsorption and desorption from the surface of the skin oil, bulk diffusion in the skin oil, stratum corneum, viable epidermis, and into the blood vessels, chemical reactions between  $O_3$  and squalene,  $O_3$  and other reactive species and reactions of products within the skin oil, stratum corneum, and viable epidermis as well as gas-phase reactions between  $O_3$  and volatile products. Production of squalene by oil glands and intercellular lipids was also treated.<sup>37</sup> Details of the differential equations included in the model describing the evolution of species within the gas phase and different layers of the skin due to mass transport, production, and loss are summarized in the Supporting Information.

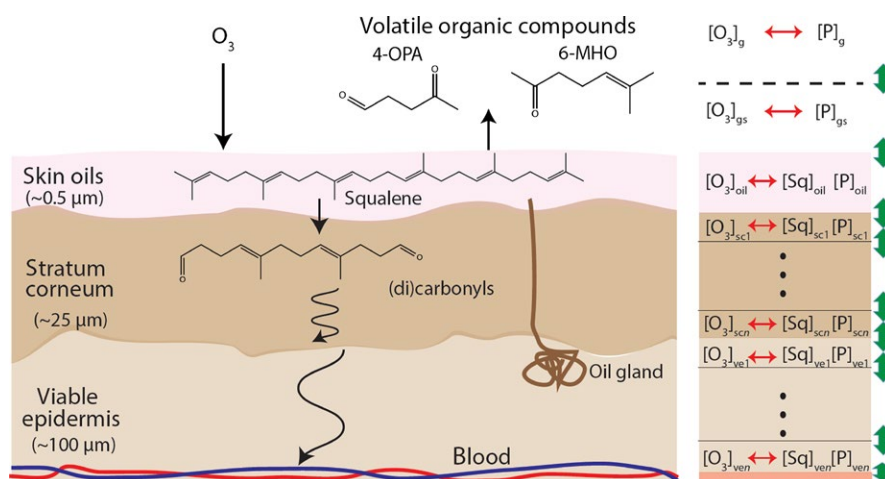


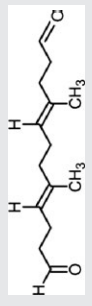
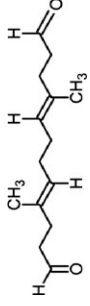
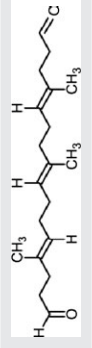
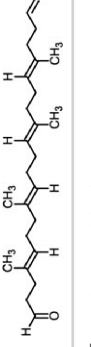
**FIGURE 1** Interactions of  $O_3$  with the skin. Reactions of  $O_3$  with skin lipids including squalene. Reaction products include gas-phase volatile organic compounds such as 4-OPA and 6-MHO as well as semi- or low-volatile products, which may diffuse through the stratum corneum and the viable epidermis to the blood. The right panel shows the schematic of the KM-SUB-Skin model developed in this study. Mass transport fluxes and chemical reactions are shown as green and red arrows, respectively. Sq and P symbolize squalene and ozonolysis products, respectively. Note that we also include other species and reactions within the model (see text for more details). The subscripts g, gs, oil, sc1, scn, ve1, and ven represent the gas phase, near-surface gas phase, oil layer, first layer of the stratum corneum, last layer of the stratum corneum, first layer of the viable epidermis, and last layer of the viable epidermis, respectively.

**TABLE 1** Squalene ozonolysis chemistry, partition coefficients, and diffusion coefficients of squalene ozonolysis products. See text for more details about how values were obtained

Structure	Name	Ozonolysis products	Vapor pressure at 298K (Pa)	Volatile/ Non-volatile <sup>a</sup>	Partition coefficient	Diffusion coefficient in the stratum corneum (cm <sup>2</sup> s <sup>-1</sup> )	Diffusion coefficient in the viable epidermis (cm <sup>2</sup> s <sup>-1</sup> )
	Squalene	Acetone, 6-MHO, Geranyl acetone, TOT, TOP, TTT	1.52×10 <sup>-4</sup>	Non-volatile	N/A	7.3×10 <sup>-18</sup>	3.4×10 <sup>-13</sup>
	Acetone	NO REACTION	3.09×10 <sup>4</sup>	Volatile	34	4.6×10 <sup>-11</sup>	3.9×10 <sup>-6</sup>
	6-MHO	4-OPA, Acetone	238	Volatile	6.3×10 <sup>5</sup>	9.7×10 <sup>-11</sup>	8.6×10 <sup>-7</sup>
	Geranyl acetone	4-OPA, 4-MON, Acetone, 6-MHO	335	Volatile	7.1×10 <sup>6</sup>	1.3×10 <sup>-10</sup>	9.7×10 <sup>-8</sup>
	TOT	Acetone, 6-MHO, Geranyl acetone, 4-OPA, 4-MON, TTT, TOP, Product A, Product C, Product D	2.26×10 <sup>-5</sup>	Non-volatile	N/A	1.9×10 <sup>-15</sup>	1.3×10 <sup>-11</sup>
	TOP	Acetone, 6-MHO, Geranyl acetone, 4-OPA, 4-MOD, TTT, Product B, Product C	1.39×10 <sup>-3</sup>	Non-volatile	N/A	1.5×10 <sup>-13</sup>	2.7×10 <sup>-10</sup>
	TTT	Acetone, 6-MHO, Geranyl acetone, 4-MOD, 1,4-butanediol, Product A	5.37×10 <sup>-2</sup>	Non-volatile	N/A	1.5×10 <sup>-11</sup>	5.4×10 <sup>-9</sup>
	4-OPA	NO REACTION	454	Volatile	4.8×10 <sup>4</sup>	5.9×10 <sup>-12</sup>	3.0×10 <sup>-6</sup>
	4-MON	4-OPA	3.19	Volatile	1.3×10 <sup>7</sup>	2.1×10 <sup>-11</sup>	1.0×10 <sup>-6</sup>
	4-MOD	4-OPA, 1,4-butanediol	4.72	Volatile	6.5×10 <sup>6</sup>	3.1×10 <sup>-11</sup>	1.0×10 <sup>-6</sup>
	1,4-butanediol	NO REACTION	697	Volatile	3.0×10 <sup>9</sup>	9.8×10 <sup>-12</sup>	3.2×10 <sup>-6</sup>

(Continues)

TABLE 1 (Continued)

Structure	Name	Ozonolysis products	Vapor pressure at 298K (Pa)	Volatile/ Non-volatile <sup>a</sup>	Partition coefficient	Diffusion coefficient in the stratum corneum (cm <sup>2</sup> s <sup>-1</sup> )	Diffusion coefficient in the viable epidermis (cm <sup>2</sup> s <sup>-1</sup> )
	Product A	4-OPA, 4-MON, 4-MOD, 1,4-butanediol	6.96×10 <sup>-2</sup>	Non-volatile	N/A	7.2×10 <sup>-11</sup>	1.4×10 <sup>-7</sup>
	Product B	4-MOD, 4-OPA	6.96×10 <sup>-2</sup>	Non-volatile	N/A	7.2×10 <sup>-11</sup>	1.4×10 <sup>-7</sup>
	Product C	4-OPA, 4-MOD, 4-MON, Product A, Product B	1.18×10 <sup>-3</sup>	Non-volatile	N/A	2.0×10 <sup>-11</sup>	1.0×10 <sup>-8</sup>
	Product D	4-OPA, 4-MON, Product A, Product C	1.68×10 <sup>-5</sup>	Non-volatile	N/A	3.4×10 <sup>-13</sup>	5.2×10 <sup>-10</sup>

<sup>a</sup>Consistent with observations from Wisthaler and Weschler<sup>6</sup> and consistent with the listed vapor pressures that were obtained from the EPIWIN Suite 4.1 software.

Table 1 summarizes the chemical structures of the squalene ozonolysis products and lists the skin-air partition coefficients as well as the diffusion coefficients in the stratum corneum and viable epidermis used in KM-SUB-Skin. Products due to the isomerization of stabilized carbonyl-O-oxides (such as hydroxy acetone and OH-6MHO) were not included in KM-SUB-Skin as these are observed only in small mixing ratios when humans are exposed to O<sub>3</sub>, compared to the products shown in Table 1.<sup>6</sup> Also not specifically included were carbonyls originating from the ozonolysis of fatty acids (e.g., decanal), although these would be one of the products of reactions of other skin chemicals and ozone (R13 in Table S1). Partition coefficients of volatile products were obtained by fitting data (as discussed below) and were consistent with the vapor pressures as obtained from the EPIWIN Suite 4.1 software such that acetone < 1,4 butanediol < 4-OPA < 6-MHO < 4-MOD < Geranyl acetone < 4-MON.

Bulk diffusion coefficients of species within the stratum corneum were calculated using the equations in Table 4 of Wang *et al.*<sup>38</sup> and ranged from 7.3×10<sup>-18</sup> cm<sup>2</sup> s<sup>-1</sup> for squalene to 1.3×10<sup>-10</sup> cm<sup>2</sup> s<sup>-1</sup> for geranyl acetone. These diffusion coefficients are consistent with the phase state of the skin<sup>39</sup>: The stratum corneum is a dehydrated layer of the skin adopting a semisolid state, whereas the viable epidermis is hydrated and much less viscous. Details about the basic model framework for the representation of the stratum corneum can be found in the previous studies.<sup>38,40</sup> Briefly, the model comprises a 'brick and mortar' arrangement of corneocytes (dead flattened cells) embedded in a lipid matrix. They used a combination of fundamental transport theory with calibrations of existing data to develop their set of equations for the transport of species through the stratum corneum. These equations include five microscopic transport properties that are necessary for describing the transport through the stratum corneum:  $D_{cor}$  (the corneocyte phase diffusivity),  $K_{cor/w}$  (the partition coefficient for a species in the corneocyte phase defined relative to the aqueous phase at a given pH),  $D_{lip}$  (the lateral diffusivity for solute motion in the plane of a lipid bilayer),  $K_{lip/w}$  (the partition coefficient for a species in the intercellular lipid phase defined relative to the aqueous phase at a given pH), and  $k_{trans}$  (the transbilayer mass transfer coefficient for motion from one bilayer to the next). These parameters were dependent upon the molecular weights, the octanol-water partition coefficient ( $K_{ow}$ ), and solute volumes of the species.  $K_{ow}$  was obtained from the EPIWIN Suite 4.1 software, whilst the solute volumes of the species were determined using the Schroeder's method as detailed in the supplementary material of Wang *et al.*<sup>38</sup> The  $K_{ow}$  values obtained from the EPIWIN software were for 25°C. However, a sensitivity test determined that the model output was not very sensitive to small changes in the value of  $K_{ow}$  (see the Supporting Information). The bulk diffusion coefficients of species within the viable epidermis were calculated using the equations of Dancik *et al.*,<sup>41</sup> resulting in 3.4×10<sup>-13</sup> cm<sup>2</sup> s<sup>-1</sup> for squalene and 3.9×10<sup>-6</sup> cm<sup>2</sup> s<sup>-1</sup> for acetone. The equations of Dancik *et al.*<sup>41</sup> were also obtained using a combination of fundamental transport theory with calibrations of existing data.

It should be noted that there is some validation of the equations of Wang *et al.*<sup>38</sup> and Dancik *et al.*<sup>41</sup>. Gong *et al.*<sup>29</sup> were able to reproduce the shapes of the cumulative absorption of *m*-xylene as well as the lag

time of ~40 minutes as measured by Kezic *et al.*<sup>42</sup> Further comparisons between the experimental measurements and modeling outputs suggest very good agreement with a maximum difference of ~20% for the maximum flux of *m*-xylene into the blood and a maximum difference of ~30% for the total amount of *m*-xylene absorbed into the blood. KM-SUB-Skin can fully reproduce the results of Gong *et al.*<sup>29</sup> for *m*-xylene absorbed into the blood when exposed to 29.4  $\mu\text{g cm}^{-3}$  of *m*-xylene as a function of exposure time (see Figure S2), confirming that mass transport is represented well in KM-SUB-Skin.

It should also be noted that the concentration of skin oils present on clothing compared to on the skin is unknown and would be dependent upon many factors including the length of time for which the clothing had been worn. A previous study has shown that clothing can account for about 70% of  $\text{O}_3$  removal from a person.<sup>18</sup> It has been demonstrated that clothing will affect the uptake of gases and that it is necessary to include the transfer of skin oil between skin and clothing within models for better predictions of dermal uptake.<sup>30,43</sup> The effect of clothing, including the evolution of skin oil on clothing over time and the impact of different types of clothing and different numbers of layers of clothing, remains a large uncertainty in terms of the chemistry and mass transport (diffusion, reversible/irreversible adsorption) occurring on and in the clothing. Thus, for simplicity, we assume in this study that all skin oil is on the skin rather than on clothing, which is equivalent to assuming a fast contact transfer between the clothing and the skin, but this aspect should be further investigated in follow-up studies.

Table S1 summarizes the reactions included in KM-SUB-Skin. For squalene, there are six double bonds available, which react equally with  $\text{O}_3$  as there is no chemical preference or steric hindrance for any of the bonds.<sup>44</sup> For simplicity, it was assumed that every double bond would react at the same rate within the skin oil, stratum corneum, and viable epidermis. The reaction rate of squalene +  $\text{O}_3$  in chloroform has been measured as  $1.25 \times 10^{-15} \text{ cm}^3 \text{ s}^{-1}$ .<sup>45</sup> This value was then optimized using global optimization (see detailed below) to be  $1.3 \times 10^{-16} \text{ cm}^3 \text{ s}^{-1}$ , which is consistent with the rate of squalene loss for pure squalene measured by Zhou *et al.*<sup>26</sup> as shown in Figure S1. The difference in the rate coefficient measured by Razumovskii and Zaikov<sup>45</sup> and used in the model could be due to skin being much more viscous than chloroform leading to the reaction starting to become diffusion-limited as per the Smoluchowski diffusion equation.<sup>46,47</sup> The reaction of  $\text{O}_3$  with double bonds is known to form Criegee biradicals, but these reaction intermediates have not been explicitly resolved and only end products are treated within the model. The yield of carbonyls was assumed to be unity, even though the true yield might be between 0.5 and 1,<sup>48</sup> as the fate or reaction rates of other products within the skin are largely unknown (see sensitivity studies in the Supporting Information).

First-order decays of squalene ozonolysis products within the skin were also included (R14–18). These decays are caused by reactions of monocarbonyls and dicarbonyls with a variety of available amino groups, aldehyde dehydrogenase, and microbes within the skin.<sup>49,50</sup> It is also known that in acidic environments carboxylic acids form which has been shown to occur in skin oil.<sup>26</sup> A sensitivity test checking the

potential impact of a change in the mechanism is described in the Supporting Information.

Gas-phase reaction rate coefficients between  $\text{O}_3$  and volatile species were obtained from the EPIWIN Suite 4.1 software. An outdoor air exchange rate was included (R21) as well as surface reactions of  $\text{O}_3$  with the room (e.g., with carpets, walls) (R20). A constant  $\text{O}_3$  production rate (R19) was included such that with no people present within the room, a constant  $\text{O}_3$  concentration of 33 ppb would be established. It should also be noted that removal of gas-phase species due to inhalation is treated as negligible as typically a human will only breathe in ~0.5–0.8  $\text{m}^3$  of air within 1 hour, which is much lower than the transport of air out of the room of ~28.5  $\text{m}^3 \text{ h}^{-1}$  in a 28.5  $\text{m}^3$  room for an air exchange rate of 1  $\text{h}^{-1}$ .

Table S2 summarizes the other input parameters including the surface area and volume of a person, the squalene concentration in the skin oil, the concentration of 'other species' in the skin oil, the production rate of squalene from the oil glands, and kinetic parameters such as the surface mass accommodation, desorption lifetime, the Henry's law constant of  $\text{O}_3$ , and the bulk diffusion coefficients of  $\text{O}_3$  in different parts of the skin. Skin concentrations were calculated using the following equation:

$$\begin{aligned} \text{Skin concentration} = & (\text{Conc. in the skin oil} \times T_{\text{oil}} \\ & + \text{Conc. in the stratum corneum} \times T_{\text{SC}} \\ & + \text{Conc. in the viable epidermis} \times T_{\text{VE}}) / (T_{\text{oil}} \\ & + T_{\text{SC}} + T_{\text{VE}}) \end{aligned} \quad (1)$$

where  $T_{\text{oil}}$ ,  $T_{\text{SC}}$ , and  $T_{\text{VE}}$  are the thicknesses of the skin oil, stratum corneum, and viable epidermis, respectively. Fluxes into the blood were determined as moles of a compound that had entered the blood per square meter of skin.

### 3 | EXPERIMENTAL DATA

The KM-SUB-Skin model was applied to three sets of experimental data. The first two sets of data (Scenario 1 and Scenario 2) were published by Wisthaler and Weschler<sup>6</sup> and consist of measurements of  $\text{O}_3$  and volatile species in a 28.5  $\text{m}^3$  chamber with two people. The third set of data (Scenario 3) consists of new measurements of volatile species that were conducted for this study. A 3.87  $\text{m}^3$  enclosure was placed on a 0.79  $\text{cm}^2$  section of a person's forehead and exposed to 72 ppb of  $\text{O}_3$  at a flow rate of 62  $\text{cm}^3 \text{ min}^{-1}$ . The evolving gas-phase species were measured using a proton transfer reaction time-of-flight mass spectrometry (PTR-TOF-MS 8000 instrument, Ionicon Analytik, Innsbruck, Austria), which has been described in detail by Jordan *et al.*<sup>51</sup> The instrument was calibrated for acetone using a dynamically diluted VOC standard (Apel-Riemer Environmental Inc., Boulder, CO, USA) with an accuracy of  $\pm 5\%$ . Instrumental response factors for 6-MHO, geranyl acetone, and 4-OPA were derived from ion-molecule collision theory<sup>52</sup> using calculated molecular properties. The accuracy of these data is  $\pm 30\%$ .



## 4 | DETERMINATION OF MODEL PARAMETERS

We constrain model parameters by fitting the model to the three different sets of experimental data described above. To find a common parameter set that could explain all scenarios, the optimization of some parameters was performed by global optimization. The applied global optimization method is a genetic algorithm (Matlab Global Optimization Toolbox, Mathworks® software), seeded with results from a uniformly sampled Monte Carlo search for faster convergence (MCGA method).<sup>53,54</sup> During the Monte Carlo search, kinetic parameters were varied within boundaries, and for each set of parameters, a correlation to the experimental data was determined. The kinetic parameter sets with highest correlation are parsed into the genetic algorithm, in which these sets of parameters were iteratively optimized in analogy to processes known from natural evolution, such as survival, recombination, and mutation.

Unknown parameters in these three scenarios included: the concentration of squalene in skin oil ( $[Sq]_{oil,1}$ ,  $[Sq]_{oil,2}$ ,  $[Sq]_{oil,3}$ ) and skin ( $[Sq]_{SC+VE,1,2,3}$ ), the concentration of other reactive species (e.g., unsaturated fatty acids, antioxidants) ( $[OS]_{oil,SC,VE}$ ), the production rate of squalene from oil glands ( $P_{SQ,1,2}$ ,  $P_{SQ,3}$ ), the average reaction rate coefficients of squalene and other reactive species with  $O_3$  ( $k_{1's}$  -  $k_{12's}$ ), reactions rate coefficients of the monocarbonyl and dicarbonyl products within the skin ( $k_{14's}$  -  $k_{18's}$ ), partition coefficients of the volatile products between the skin and the gas phase ( $K$ ), reaction rate coefficients between  $O_3$  and the furnishings within the room ( $k_{20}$ ), and the amount of skin oils on the skin compared to on clothing. In Scenario 2, there could also be uncertainty in the homogeneity of the  $O_3$  throughout the room and a changing reaction rate constant of  $O_3$  with the room walls and furnishings, as the reactivity would be expected to be higher when the room was first exposed to  $O_3$  due to adsorption onto and reaction with fresh surfaces.

We optimized only the most uncertain and important parameters (as determined from sensitivity tests) using the MCGA method. Whenever possible, we optimized these parameters around literature values. When no *a priori* information was available, we optimized the parameters around values obtained during a preliminary fitting. Partition coefficients were obtained by a preliminary fitting of Scenario 3, which indicated that the shape of the data (i.e., the constant increase in geranyl acetone concentrations and the increase in 6-MHO concentrations over the first 200 seconds followed by a steady concentration) could only be explained with the partition coefficients shown in Table 1. Concentrations of squalene and other reactive species determined by global optimization are actually effective concentrations as these species are not necessarily only within the skin oil and skin but may also be on clothing, hair, etc. The sensitivity tests for the optimized parameters are described in detail in the supplementary information.

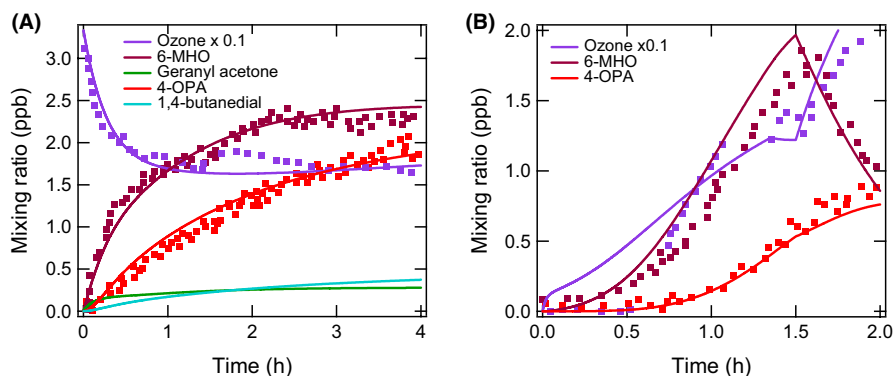
## 5 | RESULTS AND DISCUSSION

Figure 2A shows Scenario 1 where two people entered the chamber with an equilibrated  $O_3$  concentration of ~33 ppb. Over the four hours that the two people remained within the chamber, the  $O_3$

concentration decreased to a new steady-state value of ~16 ppb, whilst the concentrations of 6-MHO and 4-OPA were measured to increase. Geranyl acetone evolved in a similar way to 6-MHO but by a factor of 8 less and 1,4-butanediol evolved in a similar way to 4-OPA, but by a factor of 5 less.<sup>6</sup> In Scenario 2, two people were present within the chamber, and subsequently, the chamber was ventilated with air containing  $O_3$ . The concentrations of  $O_3$ , 6-MHO and 4-OPA then increased. After ninety minutes, the two people exited the chamber and the  $O_3$  and 4-OPA concentrations continued to increase over the next 30 minutes of measurements, whereas the 6-MHO concentrations decreased (Figure 2B). In Scenario 3, over the exposure time acetone and 6-MHO concentrations rapidly stabilized to concentrations of ~15 ppb and ~11 ppb, respectively, whilst geranyl acetone and 4-OPA concentrations slowly increased to ~3 ppb and ~0.2 ppb, respectively, as shown in Figure 3.

As shown by the solid lines in Figures 2 and 3, KM-SUB-Skin can reproduce the experimental data very well. These model results facilitate a better understanding of the concentrations of different species within the three model scenarios. For example, 4-OPA is present at much higher concentrations compared to geranyl acetone in Scenario 1, whilst in Scenario 3, the opposite trend is observed. This is due to gas phase reactions being very important in Scenario 1, with the majority of volatile dicarbonyls being produced in the gas phase rather than in the skin. In comparison, the significantly shorter residence time of gas-phase species in Scenario 3 means that monocarbonyls do not have the time to react with  $O_3$  forming dicarbonyls within the gas phase. The rapid formation of dicarbonyls in the gas phase can also be observed in Scenario 2, where 4-OPA concentrations continue to increase rapidly over the 30 minutes after people exited the room at 1.5 hours.

Figure 4 shows the temporal evolution of  $O_3$ , squalene, monocarbonyls, and dicarbonyls within the skin oil, stratum corneum, and viable epidermis for Scenario 1. The concentration of squalene slowly decreases within the skin oil over the four hours reaching ~10% of its initial value, whilst  $O_3$  monocarbonyls and dicarbonyls rapidly establish steady-state concentrations of  $\sim 5 \times 10^{12} \text{ cm}^{-3}$ ,  $\sim 1 \times 10^{18} \text{ cm}^{-3}$ , and  $1 \times 10^{17} \text{ cm}^{-3}$ , respectively. Although the thickness of the viable epidermis is considerably greater than the thickness of the stratum corneum, the diffusion through the stratum corneum is markedly slower than that in the hydrated viable epidermis, making it the main diffusion barrier of the human body to incoming gases.<sup>55</sup> Concentrations of  $O_3$  penetrating into the skin and diffusing into the blood were found to be negligible due to fast reactions in the skin oil and the top micrometer of the stratum corneum. This is consistent with an estimated  $O_3$  reacto-diffusive length in the skin oil of ~2.5  $\mu\text{m}$  and in the stratum corneum of ~0.3  $\mu\text{m}$ . Reacto-diffusive lengths represent the average distance that a species will travel from a surface before reacting and are calculated as  $(D/k^l)^{0.5}$ , where  $k^l$  is the first-order or pseudo first-order reaction constant and  $D$  is the diffusion coefficient.<sup>56,57</sup> Similarly, dicarbonyls were reacted away in the stratum corneum. Larger concentration gradients were observed in the stratum corneum for monocarbonyls due to the smaller diffusion coefficients leading to products in the stratum corneum being not as well mixed as in the viable epidermis. However, note that the temporal evolution of the products



**FIGURE 2** Observed gas-phase concentrations of ozone and volatile species upon exposing two people to  $O_3$  in a  $28.5\text{ m}^3$  room at an ambient temperature of  $23^\circ\text{C}$ . (A) Scenario 1: Two people enter a room with an equilibrated  $O_3$  concentration of 33 ppb. Geranyl acetone was measured to evolve in a similar way to 6-MHO, but a factor of 8 less and 1,4-butanediol was measured to evolve in a similar way to 4-OPA, but a factor of 5 less. (B) Scenario 2:  $O_3$  generation occurs at time 0 into the room containing two people, and after 1.5 hours, the two people exit the room. Data points are from,<sup>6</sup> whereas lines are modeled by KM-SUB-Skin.

through the skin is highly dependent upon the rate constants of reactions R14–R18, which were some of the largest uncertainties within the model and further measurements are required to better constrain these parameters.

Table S4 summarizes the predicted gas-phase and skin concentrations and fluxes into the blood of the 14 squalene ozonolysis products for Scenario 1 as well as an estimate of the loss rates of products within the skin due to reactions R14–18 which could potentially cause harm. To our knowledge, these are the first estimations of concentrations in the skin and fluxes into the blood of squalene ozonolysis products due to people being exposed to  $O_3$  within a room; although as stated above, it is likely that there are some errors associated with these numbers. After one hour of  $O_3$  exposure, non-volatile monocarbonyls (TOT, TOP, and TTT) are expected to be the dominant products in the skin followed by geranyl acetone and 6-MHO. Geranyl acetone and 6-MHO are the only products expected to have a significant flux into the blood. This is due to a combination of relatively fast diffusion coefficients through the stratum corneum compared to other products as well as relatively high partition coefficients and slow first-order rate losses within the skin.

Although the skin irritation potential of most of products remains unknown, it has been established that geranyl acetone can cause skin irritation, whilst dicarbonyls have previously been identified as skin irritants and sensitizers.<sup>21,27</sup> Figure 5 shows the predicted monocarbonyl and dicarbonyl fluxes into the blood as well as the total amounts absorbed into the blood of a single person for Scenario 1. Figure 4A shows that after 4 hours the flux of monocarbonyls into the blood would reach  $\sim 0.085\text{ ng m}^{-2}\text{ min}^{-1}$ , whilst the dicarbonyl flux would be significantly lower due to the rapid reactions of dicarbonyls with skin components. We were also able to predict that after 4 hours,  $\sim 24\text{ ng}$  of monocarbonyls and  $5 \times 10^{-9}\text{ ng}$  of dicarbonyls would have entered the bloodstream of each of the people present in the room.

We also investigated the effect on Scenario 1 of changing the number of people in the room, the  $O_3$  concentration, the size of the room, and the air exchange rate. For all scenarios listed below, only a single parameter was varied and all others kept constant (and

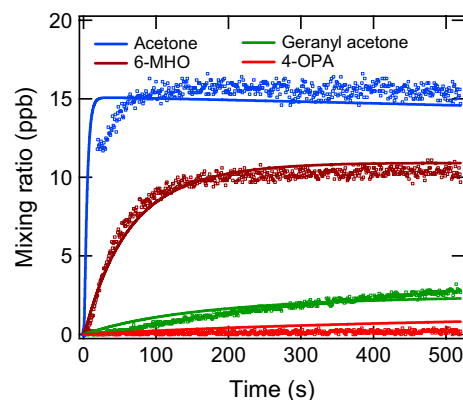


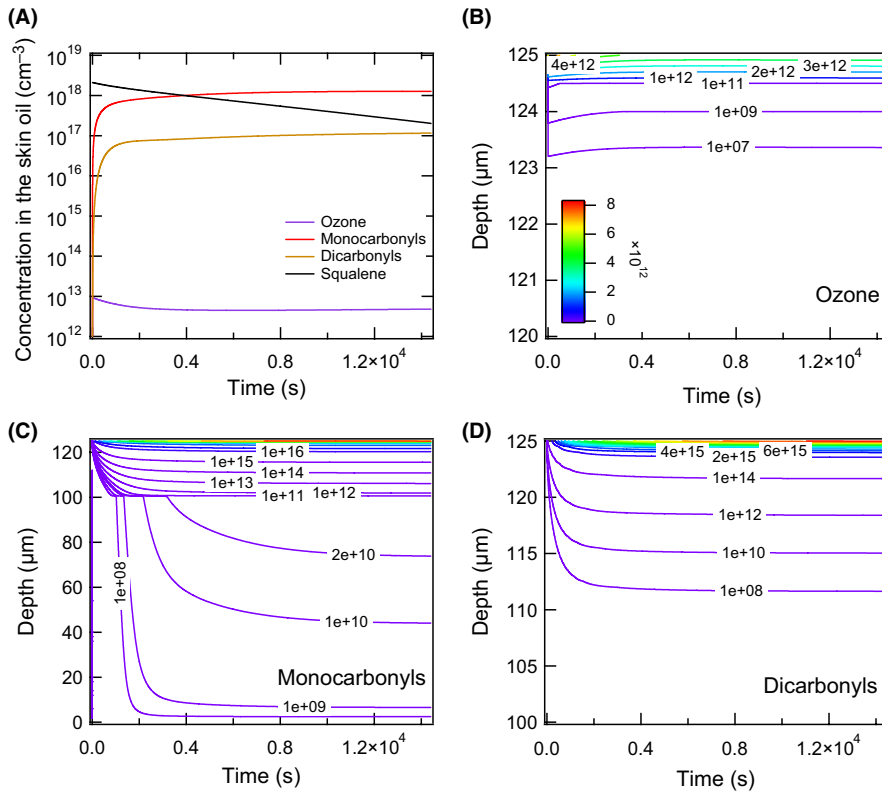
**FIGURE 3** Scenario 3: Observed volatile species (acetone, geranyl acetone, 6-MHO, 4-OPA), when a  $3.87\text{ cm}^3$  enclosure was placed on a  $0.79\text{ cm}^2$  section of a person's forehead and exposed to 72 ppb of  $O_3$  at a flow rate of  $62\text{ cm}^3\text{ min}^{-1}$ . Lines are modeled by KM-SUB-Skin. The data points are new measurements obtained in this study.

the same as for Scenario 1) and can be found in Tables 1 and S1–2. It should be noted that these are extrapolations of Scenario 1 and that uncertainties exist due to uncertainties in the model (as discussed above) and the results should be treated as semi-quantitative. However, the general trends of the results shown below should be estimated correctly.

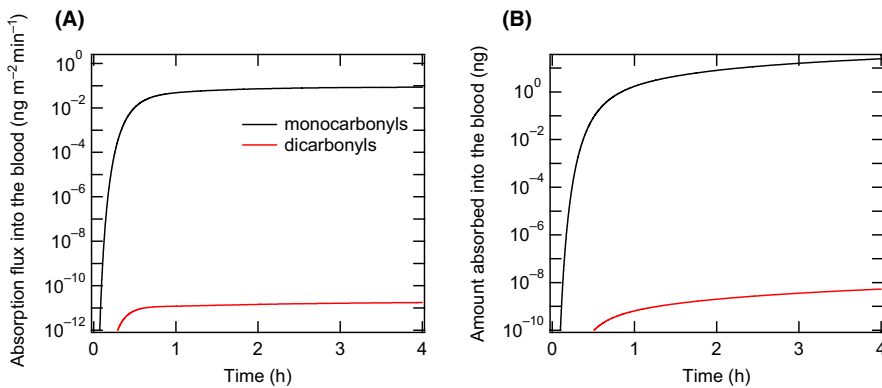
## 5.1 | Number of people in the room

Figure 6A shows the effect of varying the number of people in a  $28.5\text{ m}^3$  room upon the  $O_3$  concentrations as well as gas phase, skin, and blood monocarbonyls and dicarbonyls. As expected, by increasing the number of people within the room the  $O_3$  concentration decreased, as the total amount of squalene and other reactive species within the room increased. Somewhat surprisingly, dicarbonyl concentrations in the gas phase decreased, whilst monocarbonyl concentrations increased reaching a maximum of  $\sim 8.7\text{ ppb}$  after 4 hours with 20 people in the room. Both skin monocarbonyl and dicarbonyl concentrations decreased, whilst monocarbonyls and





**FIGURE 4** Temporal evolution of (A) O<sub>3</sub>, monocarbonyls, and dicarbonyls in the skin oil and bulk concentration profiles of (B) O<sub>3</sub> (C) monocarbonyls and (D) dicarbonyls in the skin for Scenario 1. In panels (B–D), the top 25 μm represents the stratum corneum and the bottom 100 μm represents the viable epidermis (unit of contour lines: cm<sup>-3</sup>).



**FIGURE 5** (A) Predicted absorption flux of monocarbonyls and dicarbonyls and (B) predicted amount of monocarbonyls and dicarbonyls absorbed into the blood of 1 person for Scenario 1.

dicarbonyl fluxes into the blood also decreased with increasing numbers of people. With the addition of each person, each individual is exposed to less O<sub>3</sub> and fewer monocarbonyls and dicarbonyls would form in the skin oil. However, the total amount of monocarbonyls and dicarbonyls formed would increase, but would be shared between the people. The initial large increase in gas-phase monocarbonyl concentrations is due to an increasing rate of O<sub>3</sub> reacting with squalene (R1), whilst dicarbonyls will decrease due to the decrease in O<sub>3</sub> concentrations (which is much more influential for dicarbonyls). The partitioning between the skin and the room is also important. The ratio of skin to volume of the room will increase with more people in the room, leading to more partitioning to the skin and hence lower concentrations in the gas phase. Fluxes of monocarbonyls and dicarbonyls into the blood show only a very slight decrease upon increasing the number of people.

## 5.2 | Size of the room

The effects of room size upon monocarbonyl and dicarbonyl gas phase, skin concentrations, and fluxes into the blood were studied with results shown in Figures 6B. O<sub>3</sub> production rates and removal rates into the room were kept constant, leading to a steady-state O<sub>3</sub> concentration of ~33 ppb in the absence of people within all room sizes. However, with two people present within the room, as the room size increased the O<sub>3</sub> concentration also increased, because people had less impact upon the O<sub>3</sub> concentrations within the room. Gas phase monocarbonyl concentrations decreased as the room size increased due to dilution of the monocarbonyls within the room. Gas phase dicarbonyls initially increased as the room size increased (room size <15 m<sup>3</sup>) due to each individual person being exposed to higher O<sub>3</sub> concentrations but then decreased as the room

size increased (room size  $>15\text{ m}^3$ ) due to dilution within the room. The flux into the blood followed a similar trend to concentrations within the gas phase, as volatile products partitioned more to the gas phase and therefore did not diffuse through the skin into the blood. Concentrations of skin monocarbonyls and dicarbonyls were influenced by  $\text{O}_3$  concentrations with concentrations of non-volatile products increasing with increasing room size, and also by semi-volatile products partitioning more into the gas phase with increasing room size.

### 5.3 | $\text{O}_3$ concentration

We investigated the effect of changing the  $\text{O}_3$  concentration within a room upon respiratory and skin irritants in two ways. Firstly, we studied the effect of increasing the  $\text{O}_3$  production rate (equivalent to the outdoor-to-indoor transport of  $\text{O}_3$ ) in the room (Figure 6C), and secondly, we investigated the effect of the removal of  $\text{O}_3$  due to surfaces within the room (e.g., walls, carpets, furniture) (Figure S3). It should be noted that higher removal of  $\text{O}_3$  to surfaces would also be expected if plants or  $\text{O}_3$  scrubbers were placed within the room.<sup>58,59</sup> As expected, by increasing the  $\text{O}_3$  production rate or decreasing the surface removal rate of  $\text{O}_3$ , the concentrations of monocarbonyls and dicarbonyls increased in the gas phase, skin, and blood. A doubling of  $\text{O}_3$  production rates increased  $\text{O}_3$  concentrations as well as carbonyls in the gas-phase, skin and blood by almost a factor of two. However, the largest impact was upon the concentrations of gas phase, skin, and blood dicarbonyls, which increased by over a factor of four. This increase in dicarbonyls is due to dicarbonyls being secondary products, whose formation requires two  $\text{O}_3$  molecules. Similarly, an increase in  $\text{O}_3$  surface removal had a larger impact on dicarbonyl concentrations than on monocarbonyl concentrations. However, at very high  $\text{O}_3$  concentrations monocarbonyl concentrations in the skin started to decrease due to squalene concentrations being depleted.

### 5.4 | The air exchange rate

The effects of varying the air exchange rate are shown in Figure 6D. We maintained a constant steady-state  $\text{O}_3$  concentration in the absence of people of 33 ppb  $\text{O}_3$  by increasing the outdoor-to-indoor transport of  $\text{O}_3$  (R19) to counterbalance the indoor to outdoor removal of  $\text{O}_3$  (R21). The results show that as the air exchange rate increased, the  $\text{O}_3$  concentration also increased as removal of  $\text{O}_3$  by people within the room was counteracted by greater outdoor-to-indoor transport of  $\text{O}_3$  (R19). However, as expected, gas phase concentrations of monocarbonyls and dicarbonyls decreased, as they were transported outside much more rapidly. Fluxes into the blood also slightly decreased, as more volatile products partitioned to the gas-phase rather than diffusing through the skin to the blood. The concentration of monocarbonyls and dicarbonyls in the skin was stable, as although volatile products partitioned more to the gas phase, a greater  $\text{O}_3$  concentration increased the concentrations of non-volatile monocarbonyls and dicarbonyls.

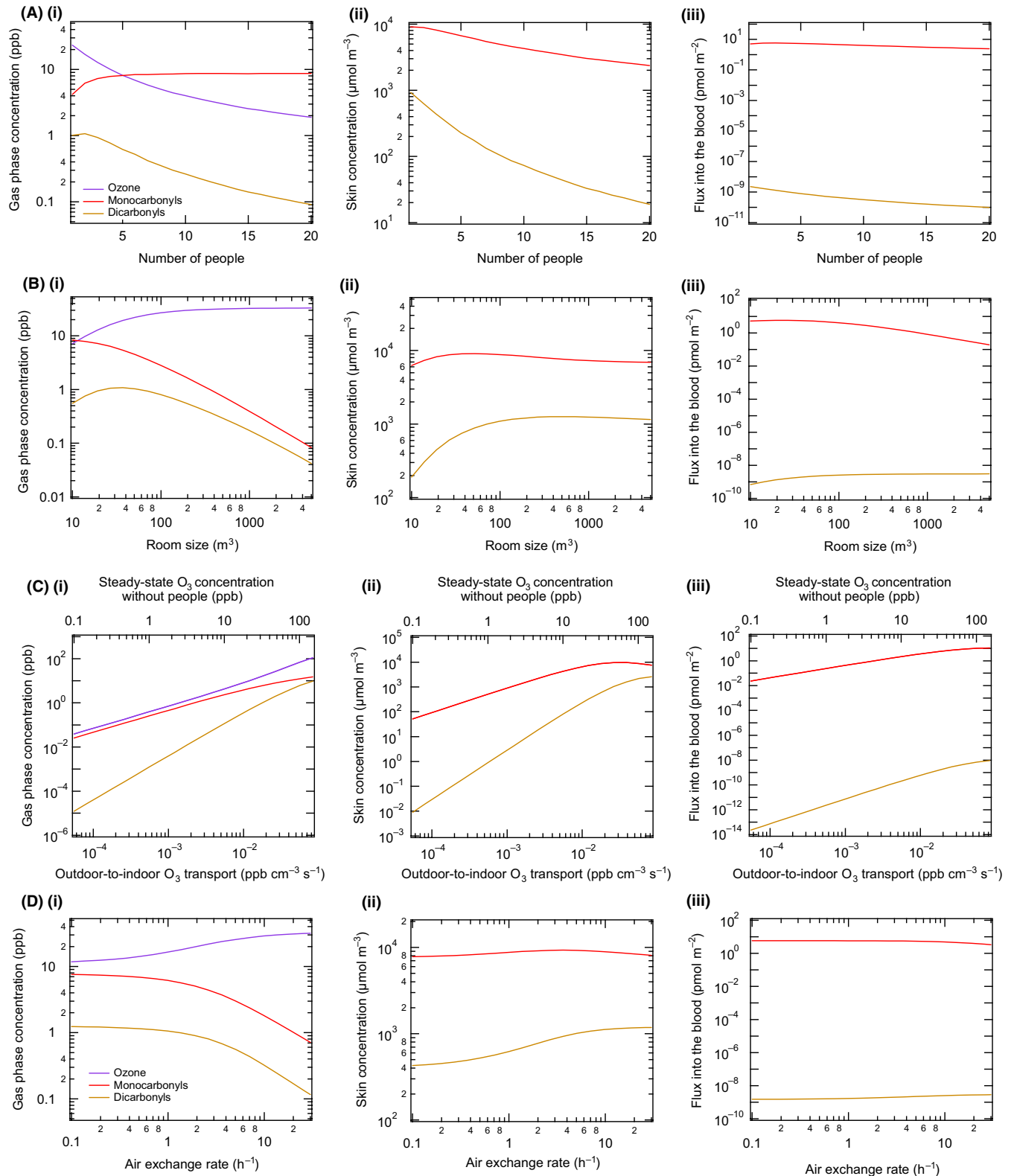
## 5.5 | Composition of monocarbonyls and dicarbonyls under different scenarios

Table S5 summarizes how the composition of the total monocarbonyls and dicarbonyls in both the gas-phase skin and blood change under different scenarios. When more partitioning to the gas phase occurs, such as when there are less people, an increase in the room size or an increase in the air exchange rate, the proportion of volatile monocarbonyls and dicarbonyls in the skin decreases. The contribution of a certain species to gas phase monocarbonyl and dicarbonyl concentrations is determined by a variety of factors with the most important factor being the partition coefficient. For example, geranyl acetone, which has the highest partition coefficient of the monocarbonyls, will contribute more to gas phase monocarbonyl concentrations compared to acetone and 6-MHO, as the air exchange rate and the room size increase.

An increase in  $\text{O}_3$  due to greater outdoor-to-indoor transport or decreased  $\text{O}_3$  surface removal leads to a greater destruction of species containing more double bonds (such as TOT and Product D), leading to a decrease in their contribution to the total monocarbonyl and dicarbonyl concentrations, respectively. An increase in  $\text{O}_3$  concentrations also leads to an increase in the contribution of acetone to monocarbonyl concentrations in the gas phase, as it is a final product that is not destroyed by  $\text{O}_3$ .

## 6 | CONCLUSIONS AND OUTLOOK

The kinetic multilayer model of surface and bulk chemistry of the skin (KM-SUB-Skin) was developed incorporating both mass transport processes and squalene ozonolysis chemistry. Model parameters were constrained using both the measurements of Wisthaler and Weschler<sup>6</sup> and a new set of data. The model enabled the first semi-quantitative estimations of monocarbonyl and dicarbonyl concentrations within the skin and fluxes into the blood as well as estimations of the concentrations of the gas-phase products generated by exposure of people to  $\text{O}_3$  in different indoor environments. The effects of changing the number of people in the room, the outdoor-to-indoor transport of  $\text{O}_3$ ,  $\text{O}_3$  removal by surfaces in the room, the size of the room, and the outdoor air exchange rate were investigated. As expected, decreasing the rate for outdoor-to-indoor transport of  $\text{O}_3$  and increasing the  $\text{O}_3$  removal rate to surfaces within the room lead to a decrease in all products in the gas phase, skin, and blood. Increasing the number of people within the room would decrease the concentrations of products in the skin and blood. Increasing the room size and air exchange rate leads to a decrease in total concentrations of products in the gas phase and blood. In any case,  $\text{O}_3$  can be scavenged by squalene very efficiently, preventing  $\text{O}_3$  penetrating into the skin and the blood. It should be noted that although these are the first estimations of squalene ozonolysis products, uncertainties still remain and that the results could vary depending on factors such as the squalene concentration, which would vary with the amount of skin oil on different individuals.



**FIGURE 6** Estimated concentrations of  $\text{O}_3$  in the gas phase (purple lines) and squalene ozonolysis products (monocarbons (red) and dicarbonyls (brown)) in the (i) gas phase, (ii) skin, and (iii) flux into the blood under different scenarios: (A) Different numbers of people. (B) Different room sizes. (C) Different outdoor-to-indoor  $\text{O}_3$  transport rates. (D) Different air exchange rates.

We note that several aspects should be implemented in future studies, which are not fully considered within the current model. A change in the ambient temperature of the room would lead to changes

in the skin temperature<sup>60</sup> and thus to changes in parameters such as  $K_{ow}$ , reaction rate coefficients, and skin/air partition coefficients. The relative humidity could also affect the chemistry that is occurring.

Whether a person uses skin creams has the potential to affect both the diffusion coefficients at the surface of the skin and the chemistry that is occurring (e.g., due to ozone reacting with antioxidants in the cream).

Another interesting factor is the skin pH; athletes and children tend to have more acidic skin, which may lead to a change in the chemistry occurring within the skin.<sup>61</sup> About 1% of the European population has the set of symptoms of a condition called ichthyosis vulgaris, whilst about 10% of the European population present mild symptoms of this condition.<sup>62</sup> This condition means that transport through the stratum corneum is faster than would be expected. The ability of skin to act as a barrier may also change with age,<sup>63</sup> affecting transdermal uptake.<sup>64</sup> Deposition velocities of O<sub>3</sub> to human occupants have been measured to vary between 0.20 and 0.62 cm s<sup>-1</sup>,<sup>30</sup> which leads to variations in O<sub>3</sub> concentrations and concentrations of squalene ozonolysis products.

Further studies with near simultaneous measurements of squalene ozonolysis products (or biomarker measurements) in both the gas phase, skin oil, skin, and blood would be required to better constrain the parameters in the model and to potentially add more complexity into our model. Additionally, the largest uncertainties within the model were due to the loss rates of squalene ozonolysis products within the skin (reactions R14-R18). Measurements of these rates and whether they vary within different regions of the skin would be extremely useful for the development of a more rigorous model.

More studies are required to determine which of the squalene ozonolysis products have the greatest respiratory and skin irritation potentials. Another interesting point is that O<sub>3</sub> could affect the nutrient source (e.g., fatty acids) of skin microbiomes (microorganisms such as viruses, bacteria, fungi, and mites) leading to a disruption in the host-microbiome relationship (dysbiosis).<sup>65-67</sup> Some of these microbiomes may play a role in fighting disease and infection of the skin, and therefore, dysbiosis could lead to a reduction in beneficial bacteria, an increase in harmful bacteria, and may even cause dermatological diseases.<sup>65,68</sup> Evidence already exists that shows that squalene by-products can lead to comedogenic skin, inflammatory acne, and possibly also wrinkling of the skin although more studies are required for a better understanding of the link between pollution, microbiomes, and skin conditions.<sup>69</sup> More studies on the interactions of atmospheric oxidants, skin components, and microbiomes are necessary before they can be incorporated into the model.

## ACKNOWLEDGEMENTS

This work was funded by the Max Planck Society. T. Berkemeier was supported by the Max Planck Graduate Center with the Johannes Gutenberg-Universität Mainz (MPGC). We thank Prof. Charles Weschler (Rutgers University) for stimulating discussion and useful comments.

## REFERENCES

1. W.H.O. *Indoor Air Pollution: National Burden of Disease Estimates*. Geneva: W.H.O.; 2007.
2. Weschler CJ. Ozone in indoor environments: concentration and chemistry. *Indoor Air*. 2000;10:269-288.
3. Morrison GC, Nazaroff WW. Ozone interactions with carpet: secondary emissions of aldehydes. *Environ Sci Technol*. 2002;36:2185-2192.
4. Rim D, Novoselec A, Morrison G. The influence of chemical interactions at the human surface on breathing zone levels of reactants and products. *Indoor Air*. 2009;19:324-334.
5. Singer BC, Coleman BK, Destailats H, et al. Indoor secondary pollutants from cleaning product and air freshener use in the presence of ozone. *Atmos Environ*. 2006;40:6696-6710.
6. Wisthaler A, Weschler CJ. Reactions of ozone with human skin lipids: sources of carbonyls, dicarbonyls, and hydroxycarbonyls in indoor air. *P Natl Acad Sci USA*. 2010;107:6568-6575.
7. Nicolaides N. Skin lipids - their biochemical uniqueness. *Science*. 1974;186:19-26.
8. Passi S, De Pità O, Puddu P, Littarru GP. Lipophilic antioxidants in human sebum and aging. *Free Radical Res*. 2002;36:471-477.
9. Thiele JJ, Traber MG, Polefka TG, Cross CE, Packer L. Ozone-exposure depletes vitamin E and induces lipid peroxidation in murine stratum corneum. *J Invest Dermatol*. 1997b;108:753-757.
10. Weber SU, Thiele JJ, Cross CE, Packer L. Vitamin C, uric acid, and glutathione gradients in murine stratum corneum and their susceptibility to ozone exposure. *J Invest Dermatol*. 1999;113:1128-1132.
11. Pöschl U, Shiraiwa M. Multiphase chemistry at the atmosphere-biosphere interface influencing climate and public health in the anthropocene. *Chem Rev*. 2015;115:4440-4475.
12. Weschler C. Chemistry in indoor environments: 20 years of research. *Indoor Air*. 2011;21:205-218.
13. Weschler C. Roles of the human occupant in indoor chemistry. *Indoor Air*. 2016;26:6-24.
14. Coleman BK, Destailats H, Hodgson AT, Nazaroff WW. Ozone consumption and volatile byproduct formation from surface reactions with aircraft cabin materials and clothing fabrics. *Atmos Environ*. 2008;42:642-654.
15. Fadeyi MO, Weschler CJ, Tham KW, Wu WY, Sultan ZM. Impact of human presence on secondary organic aerosols derived from ozone-initiated chemistry in a simulated office environment. *Environ Sci Technol*. 2013;47:3933-3941.
16. Pandrangi LS, Morrison GC. Ozone interactions with human hair: ozone uptake rates and product formation. *Atmos Environ*. 2008;42:5079-5089.
17. Rai A, Guo B, Lin CH, Zhang J, Pei J, Chen Q. Ozone reaction with clothing and its initiated VOC emissions in an environmental chamber. *Indoor Air*. 2014;24:49-58.
18. Tamas G, Weschler CJ, Bako-Biro Z, Wyon DP, Strøm-Tejsten P. Factors affecting ozone removal rates in a simulated aircraft cabin environment. *Atmos Environ*. 2006;40:6122-6133.
19. Weschler CJ, Wisthaler A, Cowlin S, et al. Ozone-initiated chemistry in an occupied simulated aircraft cabin. *Environ Sci Technol*. 2007;41:6177-6184.
20. Wisthaler A, Tamás G, Wyon DP, et al. Products of ozone-initiated chemistry in a simulated aircraft environment. *Environ Sci Technol*. 2005;39:4823-4832.
21. Anderson SE, Franko J, Jackson LG, Wells J, Ham JE, Meade B. Irritancy and allergic responses induced by exposure to the indoor air chemical 4-oxopentanal. *Toxicol Sci*. 2012;127:371-381.
22. Anderson SE, Wells J, Fedorowicz A, Butterworth LF, Meade B, Munson AE. Evaluation of the contact and respiratory sensitization potential of volatile organic compounds generated by simulated indoor air chemistry. *Toxicol Sci*. 2007;97:355-363.
23. Rai AC, Guo B, Lin C-H, Zhang J, Pei J, Chen Q. Ozone reaction with clothing and its initiated particle generation in an environmental chamber. *Atmos Environ*. 2013;77:885-892.
24. Wang C, Waring MS. Secondary organic aerosol formation initiated from reactions between ozone and surface-sorbed squalene. *Atmos Environ*. 2014;84:222-229.

25. Waring M. Secondary organic aerosol in residences: predicting its fraction of fine particle mass and determinants of formation strength. *Indoor Air*. 2014;24:376–389.
26. Zhou S, Forbes MW, Katrib Y, Abbatt JP. Rapid oxidation of skin oil by ozone. *Environ Sci Technol Lett*. 2016;3:170–174.
27. Azadi S, Klink KJ, Meade BJ. Divergent immunological responses following glutaraldehyde exposure. *Toxicol Appl Pharm*. 2004;197:1–8.
28. Thiele JJ, Podda M, Packer L. Tropospheric ozone: an emerging environmental stress to skin. *Biol Chem*. 1997a;378:1299–1306.
29. Gong M, Zhang Y, Weschler CJ. Predicting dermal absorption of gas-phase chemicals: transient model development, evaluation, and application. *Indoor Air*. 2014;24:292–306.
30. Morrison GC, Weschler CJ, Bekö G. Dermal uptake directly from air under transient conditions: advances in modeling and comparisons with experimental results for human subjects. *Indoor Air*. 2016;26:913–924.
31. Shiraiwa M, Pfrang C, Pöschl U. Kinetic multi-layer model of aerosol surface and bulk chemistry (KM-SUB): the influence of interfacial transport and bulk diffusion on the oxidation of oleic acid by ozone. *Atmos Chem Phys*. 2010;10:3673–3691.
32. Kligman AM. The uses of sebum. *Brit J Dermatol*. 1963;75:307–319.
33. Greene RS, Downing DT, Pochi PE, Strauss JS. Anatomical variation in the amount and composition of human skin surface lipid. *J Invest Dermatol*. 1970;54:240–247.
34. Weschler CJ, Nazaroff W. SVOC exposure indoors: fresh look at dermal pathways. *Indoor Air*. 2012;22:356–377.
35. Egawa M, Hirao T, Takahashi M. *In vivo* estimation of stratum corneum thickness from water concentration profiles obtained with Raman spectroscopy. *Acta Derm-Venerol*. 2007;87:4–8.
36. Reddy MB, Guy RH, Bunge AL. Does epidermal turnover reduce percutaneous penetration? *Pharmaceut Res*. 2000;17:1414–1419.
37. Sakuma TH, Maibach HI. Oily skin: an overview. *Skin Pharmacol Physiol*. 2012;25:227–235.
38. Wang TF, Kasting GB, Nitsche JM. A multiphase microscopic diffusion model for stratum corneum permeability. II. Estimation of physicochemical parameters, and application to a large permeability database. *J Pharm Sci*. 2007;96:3024–3051.
39. Shiraiwa M, Ammann M, Koop T, Pöschl U. Gas uptake and chemical aging of semisolid organic aerosol particles. *P Natl Acad Sci USA*. 2011;108:11003–11008.
40. Wang TF, Kasting GB, Nitsche JM. A multiphase microscopic diffusion model for stratum corneum permeability. I. Formulation, solution, and illustrative results for representative compounds. *J Pharm Sci*. 2006;95:620–648.
41. Dancik Y, Miller MA, Jaworska J, Kasting GB. Design and performance of a spreadsheet-based model for estimating bioavailability of chemicals from dermal exposure. *Adv Drug Deliver Rev*. 2013;65:221–236.
42. Kezic S, Janmaat A, Krüse J, Monster AC, Verberk MM. Percutaneous absorption of m-xylene vapour in volunteers during pre-steady and steady state. *Toxicol Lett*. 2004;153:273–282.
43. Morrison GC, Weschler CJ, Bekö G, et al. Role of clothing in both accelerating and impeding dermal absorption of airborne SVOCs. *J Exposure Sci Environ Epidemiol*. 2016;26:113–118.
44. Nunes FMN, Veloso M, Pereira PDP, De Andrade J. Gas-phase ozonolysis of the monoterpenoids (S)-(+)-carvone,(R)-(-)-carvone,(-)-carveol, geraniol and citral. *Atmos Environ*. 2005;39:7715–7730.
45. Razumovskii S, Zaikov G. Effect of structure of an unsaturated compound on rate of its reaction with ozone. *J Gen Chem USSR*. 1972;8:468–472.
46. Lapidus LJ, Eaton WA, Hofrichter J. Measuring the rate of intramolecular contact formation in polypeptides. *P Natl Acad Sci USA*. 2000;97:7220–7225.
47. Scheider W. Two-body diffusion problem and applications to reaction kinetics. *J Phys Chem*. 1972;76:349–361.
48. Fooshee DR, Aiona PK, Laskin A, Laskin J, Nizkorodov SA, Baldi PF. Atmospheric oxidation of squalene: molecular study using COBRA modeling and high-resolution mass spectrometry. *Environ Sci Technol*. 2015;49:13304–13313.
49. Esterbauer H, Schaur RJR, Zollner H. Chemistry and biochemistry of 4-hydroxynonenal, malonaldehyde and related aldehydes. *Free Radical Bio Med*. 1990;11:81–128.
50. Rizzo WB. Fatty aldehyde and fatty alcohol metabolism: review and importance for epidermal structure and function. *BBA -Mol Cell Biol L*. 2014;1841:377–389.
51. Jordan A, Haidacher S, Hanel G, et al. A high resolution and high sensitivity proton-transfer-reaction time-of-flight mass spectrometer (PTR-TOF-MS). *Int J Mass Spectrom*. 2009;286:122–128.
52. Su T. Parametrization of kinetic energy dependences of ion-polar molecule collision rate constants by trajectory calculations. *J Chem Phys*. 1994;100:4703.
53. Arangio AM, Slade JH, Berkemeier T, Pöschl U, Knopf DA, Shiraiwa M. Multiphase chemical kinetics of OH radical uptake by molecular organic markers of biomass burning aerosols: humidity and temperature dependence, surface reaction and bulk diffusion. *J Phys Chem A*. 2015;119:4533–4544.
54. Berkemeier T, Huisman AJ, Ammann M, Shiraiwa M, Koop T, Pöschl U. Kinetic regimes and limiting cases of gas uptake and heterogeneous reactions in atmospheric aerosols and clouds: a general classification scheme. *Atmos Chem Phys*. 2013;13:6663–6686.
55. Bouwstra J, Dubbelaar F, Gooris G, Ponc M. The lipid organisation in the skin barrier. *Acta Derm-Venerol*. 2000;208:23–30.
56. Hanson DR, Ravishankara A, Solomon S. Heterogeneous reactions in sulfuric acid aerosols: a framework for model calculations. *J Geophys Res - Atmos*. 1994;99:3615–3629.
57. Schwartz S, Freiberg J. Mass-transport limitation to the rate of reaction of gases in liquid droplets: application to oxidation of SO<sub>2</sub> in aqueous solutions. *Atmos Environ*. 1981;15:1129–1144.
58. Chameides WL. The chemistry of ozone deposition to plant leaves: role of ascorbic acid. *Environ Sci Technol*. 1989;23:595–600.
59. Fick J, Pommer L, Andersson B, Nilsson C. Ozone removal in the sampling of parts per billion levels of terpenoid compounds: an evaluation of different scrubber materials. *Environ Sci Technol*. 2001;35:1458–1462.
60. Liu Y, Wang L, Liu J, Di Y. A study of human skin and surface temperatures in stable and unstable thermal environments. *J Therm Biol*. 2013;38:440–448.
61. Schmid-Wendtner M-H, Korting HC. The pH of the skin surface and its impact on the barrier function. *Skin Pharmacol Physiol*. 2006;19:296–302.
62. Mclean WHI. The allergy gene: how a mutation in a skin protein revealed a link between eczema and asthma. *F1000 Medicine Reports*. 2011;3:2.
63. Lueberding S, Krueger N, Kerscher M. Age-related changes in skin barrier function - quantitative evaluation of 150 female subjects. *Int J Cosmet Sci*. 2013;35:183–190.
64. Weschler CJ, Bekö G, Koch HM, et al. Transdermal uptake of diethyl phthalate and di (n-butyl) phthalate directly from air: experimental verification. *Environ Health Perspect*. 2015;123:928.
65. Grice EA, Segre JA. The skin microbiome. *Nat Rev Microb*. 2011;9:244–253.
66. James A, Casey J, Hyliands D, Mycock G. Fatty acid metabolism by cutaneous bacteria and its role in axillary malodour. *World J Microb Biot*. 2004;20:787–793.
67. Naik S, Bouladoux N, Wilhelm C, et al. Compartmentalized control of skin immunity by resident commensals. *Science*. 2012;337:1115–1119.
68. Mańkowska-Wierzbicka D, Karczewski J, Dobrowolska-Zachwieja A, Adamski Z. The microbiome and dermatological diseases. *Postępy Hig Med Dosw (online)*. 2015;69:978–985.

69. Pham DM, Boussouira B, Moyal D, Nguyen Q. Oxidization of squalene, a human skin lipid: a new and reliable marker of environmental pollution studies. *Int. J Cosmetic Sci*; 2015;37:357-365.

#### SUPPORTING INFORMATION

Additional Supporting Information may be found online in the supporting information tab for this article.

**How to cite this article:** Lakey PSJ, Wisthaler A, Berkemeier T, Mikoviny T, Pöschl U, and Shiraiwa M. Chemical kinetics of multiphase reactions between ozone and human skin lipids: Implications for indoor air quality and health effects. *Indoor Air* 2016;00:1-13. doi:10.1111/ina.12360